

Determination of silver(I) ion based on the aggregation of gold nanoparticles caused by silver-specific DNA, and its effect on the fluorescence of Rhodamine B

Shenshan Zhan · Hanchu Xu · Xuejia Zhan ·
Yuangen Wu · Lumei Wang · Jing Lv · Pei Zhou

Received: 25 November 2014 / Accepted: 17 February 2015 / Published online: 11 March 2015
© Springer-Verlag Wien 2015

Abstract We report on an “off-on” type of fluorescent assay for silver(I) ion determination that is based on the use of silver-specific DNA, gold nanoparticles, and Rhodamine B (RhoB). The random coil cytosine-rich silver-specific DNA undergoes structural transformation on capturing Ag(I), and this results in a change in the aggregation status of the gold nanoparticles and simultaneously affects the fluorescence intensity of RhoB that was added to the solution. The fluorescence intensity of RhoB is related to the concentration of Ag(I) in the 2.73 to 1500 ppb range, and the detection limit is 2.73 ppb. The method was applied to the determination of Ag(I) in (spiked) water samples. Conceivably, it also may be applied to fluorescence imaging silver ions and, by using other ion-specific DNAs, to detect other metal ions.

Keywords Silver determination · Fluorescent assay · Silver-specific DNA · Rhodamine B · Gold nanoparticles

Shenshan Zhan and Hanchu Xu contributed equally to this work.

Electronic supplementary material The online version of this article (doi:10.1007/s00604-015-1462-3) contains supplementary material, which is available to authorized users.

S. Zhan · H. Xu · X. Zhan · L. Wang · J. Lv · P. Zhou (✉)
School of Environmental Science and Engineering; Key Laboratory of Urban Agriculture (South), Ministry of Agriculture; School of Agriculture and Biology, and Bor S. Luh Food Safety Research Center, Shanghai Jiao Tong University, Shanghai 200240, People's Republic of China
e-mail: peizhoujtu@163.com

Y. Wu
Guizhou Province Key Laboratory of Fermentation Engineering and Biopharmacy; School of Liquor & Food Engineering, Guizhou University, Guiyang, 550025 Huaxi District, Guizhou, People's Republic of China

Introduction

Environmental pollution caused by heavy metal ions has become an important worldwide concern [1]. Because of the increasingly common use of silver in macro-usages such as battery, bearing, brazing and soldering production, as well as in the automobile, electronics, photographic, pharmaceutical and imaging industries [2], pollution by silver(I) ions has also received extensive attention [3]. Despite not being a bioaccumulative toxin, Ag⁺ absorbed by human does inactivate sulfhydryl enzymes, bind to amino, imidazole and carboxy groups of various metabolites, and displace essential metal ions such as Ca²⁺ and Zn²⁺ in hydroxyapatite in bone [4, 5], leading to argyria and symptoms such as headache, skin irritation, stomach distress, organ edema, and even death [6]. Therefore, Ag⁺ has been assigned to the highest toxicity class, surpassed only by Hg²⁺, and rapid and sensitive detection of it has been of large interest [7].

Among the available conventional techniques, atomic absorption spectroscopy (AAS) [8], electrothermal atomic absorption spectrometry (ETAAS) [9], inductively coupled plasma atomic emission spectrometry (ICP-AES) [10], inductively coupled plasma mass spectrometry (ICP-MS) [11], voltammetry [12] and potentiometry [13] are the most commonly used for Ag⁺ detection. Respectable advantages such as high accuracy and excellent sensitivity showed by these techniques, but their wide applications in routine Ag⁺ detections remain limited due to the disadvantages of needing expensive sophisticated instruments, elaborate sample preparation, well-trained personnel and time consuming procedures [14]. So much focus has been turned to developing new methods which are simple and low cost.

Recent years have witnessed the rapid development of using functional nucleic acids as the molecular recognition

elements for the detection of metal ions [15–17]. Generally, the functional nucleic acids include aptamer, DNAzyme, G-quadruplex binding ligand and specific DNA that can selectively bind to its targets [18]. As for Ag^+ detections, the most impressive and widely used functional nucleic acid is silver-specific DNA which is rich in cytosine (C) and readily forms a hairpin structure in the C-Ag⁺-C configuration in the presence of the target Ag^+ [19]. Since Ono et al. firstly reported the selective capture of Ag^+ by C-C mismatches [20], several C-rich oligonucleotides have been designed as silver-specific DNA and omnifarious silver-specific DNA-based methods have been developed for Ag^+ detections by transforming the formation of C-Ag⁺-C base pairs into colorimetric [21], scattering [19], fluorescent [22–24] and electrochemical [25] signal output. Among these different kinds of signal output, fluorimetry occupies a considerable proportion due to its operational simplicity, high sensitivity and real-time detection [26, 27]. And those fluorescent probes for Ag^+ could be divided into two types: “off-on” type, fluorescence enhanced upon Ag^+ binding; “on-off” type, fluorescence weakened upon Ag^+ binding. It is generally acknowledged that the former type is superior compared to the latter type due to its better overall signal processing in biosystems and specificity of mode of action [28]. However, as the Ag^+ belongs to the so-called “silent ions”, the design of “off-on” type probes for it remains challenging and attractive up to now [29]. Therefore, much effort should be devoted to the development of highly selective fluorescent “turn on” probes for Ag^+ [30].

In this study, a sensitive Ag^+ quantitative method that utilized silver-specific DNA, gold nanoparticles (AuNPs) and Rhodamine B (RhoB) was presented. As shown in Scheme 1, when no target (i.e. Ag^+) exists, the silver-specific DNA that named Ag-CC can absorb onto the surface of AuNPs, and the DNA-absorbed AuNPs can maintain dispersion even at a high concentration of NaNO_3 , greatly quenching the fluorescence of RhoB. However, after the Ag-CC interacts with Ag^+ to form C-Ag⁺-C base pairs, it changes its conformation from a random coil to a hairpin structure, failing to absorb onto the AuNPs. Thus the AuNPs stay bare and aggregate induced by NaNO_3 , consequently their effect on the fluorescence of RhoB gets weak. As the fluorescence intensity of RhoB was controlled by the aggregation degree of the AuNPs, which was mediated by the silver-specific DNA, and the DNA amount that plays a

part in mediating the AuNPs correlates with the involved Ag^+ , a fluorescent assay for Ag^+ detection in aqueous solution was thus established.

Materials and methods

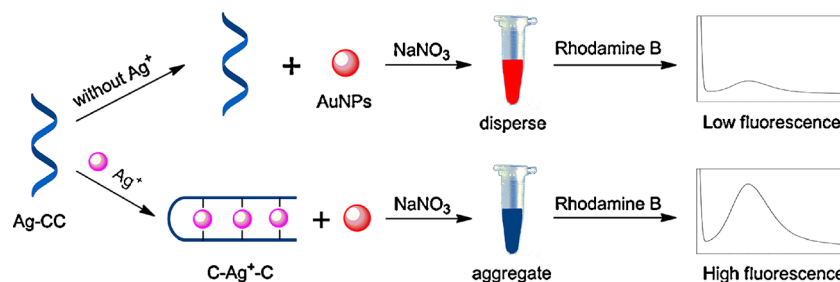
Chemicals and reagents

The sequence of the silver-specific DNA (i.e. Ag-CC) is referred to previous literature [19], and it was synthesized by Sangon Biotechnology Inc. (Shanghai, China. www.sangon.com). Its sequence is 5'-CTCTCTCTCTTCATTTTCAACACAACACAC-3' (32-mer). HAuCl_4 and 3-(N-morpholino) propanesulfonic acid (MOPS) were obtained from Sangon Biotechnology Inc., too (www.sangon.com). Rhodamine B, trisodium citrate, sodium chloride, sodium hydrosulfide, organic compounds used in selectivity study and cationic compounds such as nitrates of Ag^+ , Na^+ , K^+ , Mg^{2+} , Ca^{2+} , Ni^{2+} , Zn^{2+} , Fe^{3+} and sulfates of Fe^{2+} , Mn^{2+} , Cu^{2+} were obtained from commercial sources and used without further purification. Standard solution (1 mg·mL⁻¹, 1000 ppm) of Pb^{2+} , Hg^{2+} and Cd^{2+} were purchased from Merck Co., Inc. (Germany, www.merck.com) and used after diluted to appropriate concentration with ultrapure water. The 96-well microplate was purchased from Thermo Fisher Scientific Inc. (Nunclon, Denmark, www.thermofisher.com). Ultrapure water that utilized to prepare all aqueous solutions was from a Millipore-MilliQ (Milli-Q plus, Millipore Inc, Bedford, MA, USA, www.millipore.com) system.

Instruments

An analytical transmission electron microscope JEM-2010HT (Hitachi, Japan, www.hitachi.com) was used to observe the images of AuNPs. A Microplate Spectro-photometer M200 Pro (Tecan Group Ltd, Switzerland, www.tecan.com) was employed to determine the aggregation degree of the AuNPs. A steady-state & time-resolved fluorescence spectrofluorometer of the QM/TM/IM model (Photon Technology International, USA, www.pti-nj.com) was applied to detect the fluorescence lifetime of the RhoB that treated differently. A PL-F2X nitrogen laser was used as the excitation source for

Scheme 1 Schematic representation of the fluorescent detection of Ag^+ in aqueous solution with Rhodamine B and silver-specific DNA mediated gold nanoparticles



lifetime measurements, with the resulting fluorescence monitored at right angles through an emission monochromator with a photomultiplier tube and strobe detector. Quartz cells (1*1 cm) were used for all spectral measurements. The obtained fluorescence intensity was normalized by dividing the intensity at each time points with the highest fluorescence intensity, and the time which the normalized intensity 1 corresponded was determined as the start time (0 ns). An F-4500 fluorescence spectrophotometer (Hitachi, Japan, www.hitachi.com) was used to record the fluorescence intensity, with the response time of 0.05 s, PMT voltage of 700 V, scan speed of 1200 nm·min⁻¹, excitation wave length of 520 nm and excitation and emission slits of 10 nm. A Thermostatic incubating device (Eppendorf, China, www.eppendorf.cn) was used to provide the different incubating temperatures at which the final solution that containing all the sensing elements was incubated when studying the influences of the temperature.

Preparation of AuNPs

The AuNPs were synthesized by sodium citrate reduction of HAuCl₄ following a literature procedure [31]. Briefly, a sodium citrate solution (1 % (w/v), 10.5 mL) was rapidly added to a boiled solution of HAuCl₄ (100 mL, 0.03 % (w/w)) under vigorous stirring. The mixed solution was boiled for 10 min and further stirred for 15 min. The resulting wine-red solution was cooled to room temperature and filtered, then stored in dark glass bottles at 4 °C for further use.

Optimization of the sensing system

The volume of each sensing system was set as 500 μL and the volume of AuNPs added to each sensing system was fixed as 250 μL. The absorbance values at 520 nm (A_{520}) and 650 nm (A_{650}) were measured, and the absorbance ratio $A=A_{650}/A_{520}$ was recorded to evaluate the aggregation degree of AuNPs. The increased absorbance ratio value $\Delta A=A-A_0$ was calculated to indicate the difference of the aggregation degree of AuNPs, in which A_0 stands for the absorbance ratio of the blank solution and A for the ions treated one. When optimize the NaNO₃ concentration, AuNPs in the sensing system was treated with NaNO₃ of increasing concentration, and the minimum NaNO₃ concentration which can fully aggregate AuNPs was chose. The Ag-CC concentration was optimized by comparing the ΔA of different sensing system in the absence and in the presence of 500 ppb Ag⁺ which contain Ag-CC of different concentration. The RhoB concentration was optimized by comparing the fluorescence intensity of different sensing system in the absence and in the presence of 800 ppb Ag⁺ which contain RhoB of different concentration. The fluorescence intensity of the blank was recorded as F_0 and that of the Ag⁺ treated one was recorded as F , and the relative

fluorescence intensity was calculated as F/F_0 , and the RhoB concentration which corresponding to the highest F/F_0 value was chose.

Procedure for Ag⁺ determination

A typical Ag⁺ analysis was realized as following steps. Firstly, 7.5 μL of Ag-CC solution (1 μM) was mixed with 10 μL Ag⁺ solution of appropriate concentration. This solution was allowed to incubate for 10 min at room temperature. Secondly, 250 μL AuNPs was added to the above prepared solution and the solution was diluted with MOPS buffer (10 mM, pH 7.0) to 430 μL, and then the solution was allowed to react for 10 min at room temperature. Finally, 30 μL of 2 M NaNO₃ and 40 μL of 100 μM RhoB were added. After incubated for another 10 min under the same condition, the fluorescence intensity of each sample was monitored. Blank experiments were carried out by replacing Ag⁺ with ultrapure water. The fluorescence intensity of the blank was recorded as F_0 and that of the Ag⁺ treated one was recorded as F , and the increased fluorescence intensity was calculated as $(F-F_0)$. To test the selectivity of the assay, other competing metal ions and a series of common organic compounds instead of Ag⁺ were added in a similar way.

Results and discussion

Sensing mechanism

The sensing system is composed of silver-specific DNA, AuNPs, NaNO₃ and RhoB, and each element is prudently selected for the determination of Ag⁺. The silver-specific DNA serves as the recognition probe, besides interacts with Ag⁺ to form C-Ag⁺-C base pairs; it mediates the aggregation status of AuNPs with the help of NaNO₃. The AuNPs were usually used as a colorimetric indicator because of its high extinction coefficients and distinct size-dependent colors, while in this assay it was their excellent quenching properties, which largely depends on their dispersed/aggregated status, that was favored [32]. The section before the addition of RhoB is exactly the constitution of the classical colorimetric assay which based on the aggregation of AuNPs. However, if the concentration of the analyte is low, inconspicuous color change will be obtained, which will affect the sensitivity of the colorimetric assay [33]. Thus RhoB was introduced to convert the colorimetric signal into fluorescent signal for the sake of improving the sensitivity.

Proof-of-concept experiments were performed to demonstrate the mechanism of this assay. As shown in Fig. 1a and b, the pure AuNPs and the silver-specific DNA-coated ones were evenly distributed and maintain disperse, which could effectively weaken the originally high fluorescence of the

RhoB (line 1, 2 and 3 in Fig. 1d). The AuNPs aggregated after Ag^+ was added (c), accompany with the decrease of their effect on the fluorescence of RhoB, under which the fluorescence of the Rho B recovered to certain extent (line 4 and 5 in Fig. 1d). These results preliminarily verify the feasibility of Ag^+ determination of this assay.

Optimization of RhoB concentration

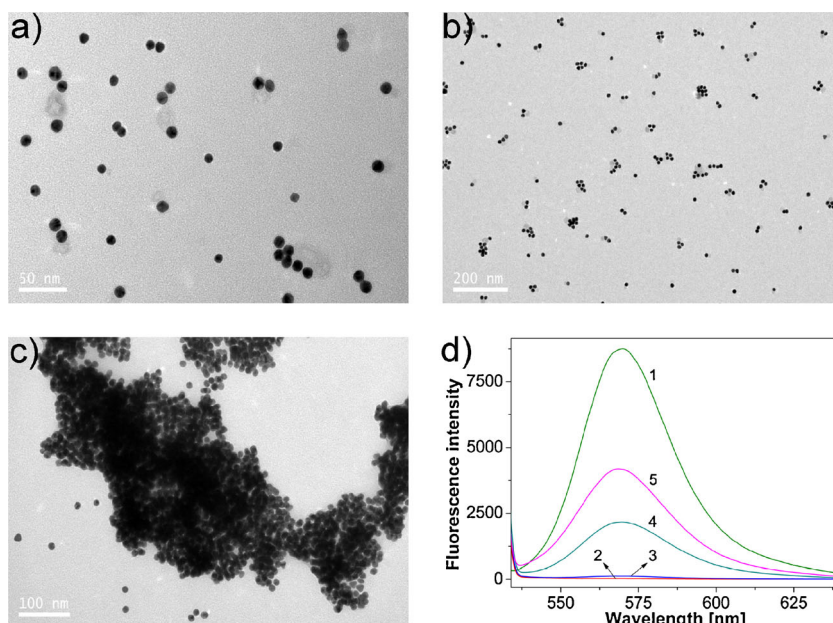
After the optimization of the NaNO_3 and Ag-CC concentration (Electronic Supplementary Material, ESM), the RhoB amount that needed was also investigated. RhoB was chosen because of its water solubility, photostability, high extinction coefficient and quantum yield [34]. RhoB molecules are highly fluorescent, but when they have been adsorbed noncovalently onto the surfaces of AuNPs through electrostatic interactions, fluorescence resonance energy transfer (FRET) and collision occur between RhoB and the AuNPs, result in almost no fluorescence emission [35]. As shown in Fig. 2, under the optimal NaNO_3 and DNA concentration, without addition of Ag^+ , a majority of the 250 μL AuNPs was supposed to maintain disperse status, and the fluorescence of RhoB were completely diminished as the RhoB concentration increases from 0 to 6 μM . When the RhoB concentration exceeds 6 μM , increasing fluorescence of RhoB appeared. When 800 ppb Ag^+ was added, fluorescence appeared even the RhoB concentration was just 4 μM . This phenomenon indicates that the introduction of Ag^+ induced the aggregation of the AuNPs, and the effect on the fluorescence of RhoB of the aggregated AuNPs was greatly weakened compared to

the dispersed ones [33]. The possible mechanism of these results may lie in two routes. One is that the surface-to-volume ratio of the aggregated AuNPs is much lower than that of the dispersed ones, thus the amounts of RhoB absorbed to the surface of aggregated AuNPs is smaller, which leads to weaker FRET between AuNPs and RhoB and decreasing quenching ability of the aggregated AuNPs [33]. The other is the fluorescence inner filter effect of AuNPs [36]. The dispersed AuNPs which has strong absorption at 520 nm can filter a part of excitation light and decrease the available emission light. While in the condition AuNPs is aggregated, the absorbance at 520 nm decreased, which leads to diminished inner filter efficient of AuNPs and more light to excite RhoB, thus more emission light is detected. The inset in the upper left shows the relative fluorescence intensity (F/F_0), it reveals that at the RhoB concentration of 8 μM , the F/F_0 obtains its maximum, which decreases as the RhoB concentration increased. In order to acquire prominent fluorescence signal and at the same time avoid high background, the optimal RhoB concentration was thus chose as 8 μM .

Study of the fluorescence lifetime

Previous studies claim that both the inner filter effect and the quenching of the dye owing to its adsorption on AuNPs contribute to the observed changes in fluorescence intensity [33, 37]. It is easy to predict the occurrence of inner filter effect as both the strong absorption of the dispersed AuNPs and the excitation wave length of the RhoB are at 520 nm. Therefore it is necessary to carry out fluorescence lifetime study to

Fig. 1 The transmission electron microscope (TEM) images of the AuNPs solutions and the fluorescence spectra of the RhoB that treated with different substances. (a) AuNPs; (b) AuNPs+15 nM Ag-CC+0.12 M NaNO_3 ; (c) AuNPs+15 nM Ag-CC+800 ppb Ag^+ +0.12 M NaNO_3 ; (d) line 1: 8 μM RhoB; line 2: 8 μM RhoB+250 μL AuNPs; line 3: 8 μM RhoB+250 μL AuNPs+15 nM Ag-CC+0.12 M NaNO_3 ; line 4: 8 μM RhoB+250 μL AuNPs+15 nM Ag-CC+800 ppb Ag^+ +0.12 M NaNO_3 ; line 5: 8 μM RhoB+250 μL AuNPs+15 nM Ag-CC+1500 ppb Ag^+ +0.12 M NaNO_3



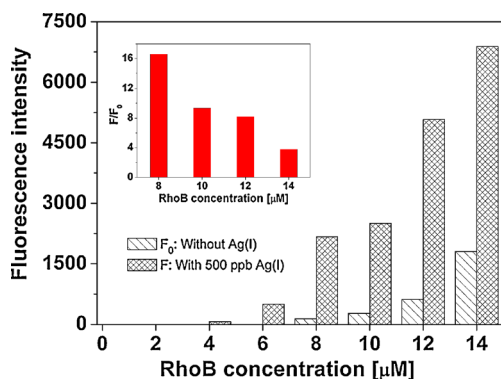


Fig. 2 The Effect of the RhoB concentration on the fluorescence intensity. The volume of AuNPs was 250 μL , the concentration of NaNO_3 was 0.12 M, and the concentration of Ag-CC was 15 nM

clarify whether the quenching of fluorescence actually happened. As shown in Fig. 3, the fluorescence decay of the RhoB that treated in different ways was monitored. The normalized fluorescence intensity of the RhoB was plotted against time by fitting to ExpDec1 plot. It could be seen that the curvature of each plot differs from those of others. The obtained fitting equation and relevant parameters were summarized in the inset, where y stands for the normalized intensity, A_1 for pre-exponential factor, x for time and t_1 for the fluorescence lifetime. It reveals that the lifetime of pure RhoB is 2.0881 ns, and when the RhoB mixed with the disperse AuNPs, its lifetime decreased to 0.6021 ns. However, if the RhoB coexists with the NaNO_3 -induced aggregate AuNPs, its lifetime mere reduced to 1.5024 ns. When RhoB treated with AuNPs which coated by Ag-CC of appropriate amount and maintained disperse status against NaNO_3 , its lifetime is 0.9111 ns. After 500 ppb Ag^+ was introduced to consume the Ag-CC and induced the aggregation of the AuNPs, the lifetime of the RhoB restores to 2.0508 ns. All these results demonstrate that the lifetime of the RhoB is affected by the aggregation degree of the AuNPs, in which dispersed AuNPs

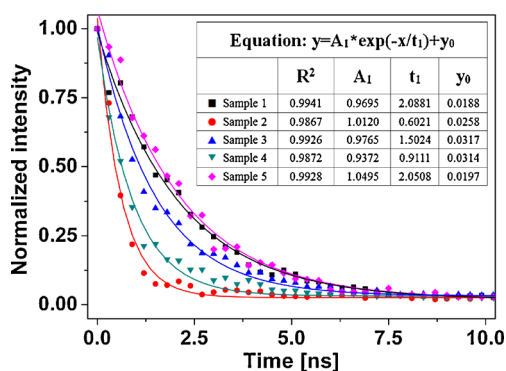


Fig. 3 Fluorescence decay profile of RhoB that treated in different ways. *Sample 1*: 8 μM RhoB; *sample 2*: 8 μM RhoB+250 μL AuNPs; *sample 3*: 8 μM RhoB+250 μL AuNPs+0.12 M NaNO_3 ; *sample 4*: 8 μM RhoB+250 μL AuNPs+15 nM Ag-CC+0.12 M NaNO_3 ; *sample 5*: 8 μM RhoB+250 μL AuNPs+15 nM Ag-CC+500 ppb Ag^+ +0.12 M NaNO_3

correspond to shorter fluorescence lifetime. As in the proof-of-concept experiments, dispersed AuNPs accompany with weaker fluorescence intensity, it thus could be concluded that the dispersed AuNPs not only decrease the fluorescence intensity of RhoB, but also reduce the fluorescence lifetime of it. These results suggest that besides inner filter effect, the fluorescence decreasing phenomenon caused by the AuNPs was also based on the quenching of fluorescence in which the lifetime is reduced by quencher [38].

Influences of temperature

In order to further elucidate the mechanism of the assay, studies have been carried out on the influences of the temperature at which the final solution that containing all the sensing elements was incubated. The results shown in Fig. 4 indicate that the increase in fluorescence intensity increased gradually as the temperature elevated from 15 to 35 $^{\circ}\text{C}$, after which the increase in fluorescence intensity rose obviously until the temperature reached 65 $^{\circ}\text{C}$, and then the increase in fluorescence intensity tends to flatten. There are mainly two reasons accounting for this phenomenon. Firstly, the Ag-CC that coated on the surface of the AuNPs would detach as the temperature increased, results in more bare AuNPs in the sensing system which would aggregate with the help of NaNO_3 . As claimed in the “optimization of RhoB concentration” section, aggregated AuNPs corresponding to weaker quenching effect on the fluorescence of RhoB, thus the breaking away of Ag-CC from surface of the AuNPs results from the increasing temperature leads to higher fluorescence intensity. Secondly, as the temperature increased to high, the non-covalent interaction between RhoB and the AuNPs may be weakened, which in turn would reduce the incidence of the FRET and collision between them, bringing about stronger fluorescence. These results further testify the mechanism of the assay. Nevertheless, as our goal is to develop assay which holds the potential

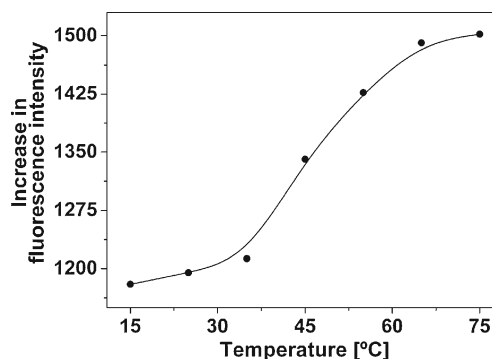


Fig. 4 The influences of the temperature on the increased fluorescence intensity of the final solution. Each sample of the final solution contains 250 μL AuNPs, 0.12 M NaNO_3 , 15 nM Ag-CC, 8 μM RhoB, 500 ppb Ag^+ and MOPS buffer (10 mM, pH 7.0) of appropriate volume

for on-site and real-time detection, room temperature (25 °C) was still used in all the following studies.

Sensitivity of the assay for Ag⁺ detection

The sensitivity of this assay was explored by measuring the fluorescence signals toward different concentration of Ag⁺. As shown in Fig. 5a, the fluorescence intensity increases as the Ag⁺ concentration increases from 0 to 1500 ppb. Figure 5b depicts the increased fluorescence intensity plotted against the concentration of Ag⁺ by fitting to a DoseResp plot with a correlation coefficient of 0.988. Inset shows the linear responses at low Ag⁺ concentrations. The slope of the linear regression equation is 0.6284 and the intersection at the y axis is 0.1044, with a correlation coefficient of 0.988. Based on previous reports [39], $3\sigma/\text{slope}$ was used to determine the limit of detection for Ag⁺ as 2.73 ppb (~25.31 nM), which is lower than that of the colorimetric assay that based on the aggregation of AuNPs [40, 41]. As the maximum contamination level for Ag⁺ in drinking water defined by the US Environmental Protection Agency (EPA) and the World Health Organization (WHO) is 50 ppb (460 nM) [19], this assay is fully applicable for Ag⁺ monitoring in drinking water. Moreover, the dynamic

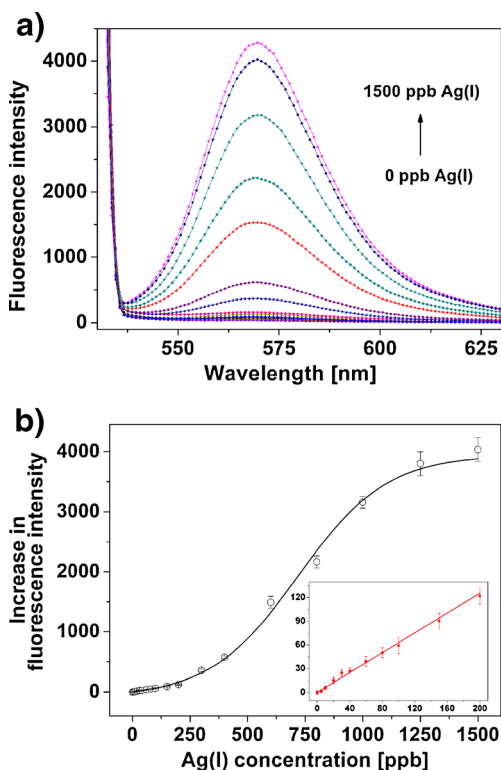


Fig. 5 **a** Fluorescence emission spectra of the sensing system on exposure to 0, 5, 10, 20, 30, 40, 60, 80, 100, 150, 200, 300, 400, 600, 800, 1000, 1250 and 1500 ppb Ag⁺. **b** Calibration curve of the sensing system for Ag⁺. Sensing system: 250 μ L AuNPs, 0.12 M NaNO₃, 15 nM Ag-CC, 8 μ M RhoB, MOPS buffer (10 mM, pH 7.0)

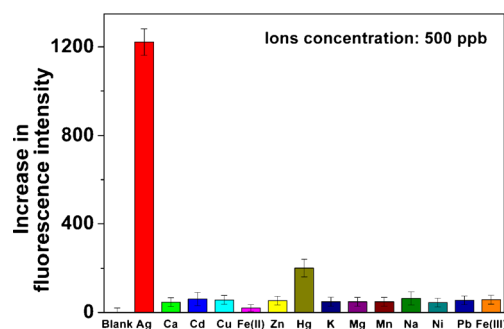


Fig. 6 Selectivity of the assay for Ag⁺ detection over other common metal ions. Ions concentrations: 500 ppb; Sensing system: 250 μ L AuNPs, 0.12 M NaNO₃, 15 nM Ag-CC, 8 μ M RhoB, MOPS buffer (10 mM, pH 7.0)

range of this assay (2.73–1500 ppb) could be simply tuned by adjusting the involved amount of Ag-CC, AuNPs and RhoB, which shows great practical utility in practical applications as the desirable concentrations for the same target analyte can be different for various applications [16].

Selectivity of the assay for Ag⁺ detection

The selectivity of the assay was investigated by carrying out control experiments by examining other metal ions, such as Ca²⁺, Cd²⁺, Cu²⁺, Fe²⁺, Zn²⁺, Hg²⁺, K⁺, Mg²⁺, Mn²⁺, Na⁺, Ni²⁺, Pb²⁺ and Fe³⁺ under identical conditions. And the results in Fig. 6 show that only Ag⁺ caused remarkable increased fluorescence intensity, other metal ions display no significant interferences. The selectivity of the assay for Ag⁺ detection over other organic compounds and other commonly existing anions, such as Cl⁻ and HS⁻ were also studied (Fig. S3 and Fig. S4, ESM). It reveals that among the testing organic compounds, except cysteine can bring slight response, other

Table 1 Determination of Ag⁺ in water samples

Samples*	Mean found (ppb)	Mean recovery (%)	RSD (%)
Ag ⁺ (200), Na ⁺ (100), Hg ²⁺ (10), Cu ²⁺ (100), Mg ²⁺ (50), Fe ²⁺ (200), NO ₃ ⁻ (649.1), SO ₄ ²⁻ (495.3)	205.3	102.7	5.21
Ag ⁺ (500), Mg ²⁺ (100), Cd ²⁺ (50), Fe ²⁺ (200), Ca ²⁺ (200), Zn ²⁺ (100), NO ₃ ⁻ (1668.8), SO ₄ ²⁻ (344.1)	504.7	100.9	3.49
Ag ⁺ (1000), K ⁺ (500), Pb ²⁺ (100), Fe ³⁺ (200), Ni ²⁺ (50), Mn ²⁺ (200), NO ₃ ⁻ (2201.7), SO ₄ ²⁻ (349.6)	998.5	99.9	4.87

* Three assays were conducted for each sample

The numbers in parentheses after each anion and cation show the final concentration [ppb] of the ions added. Concentrations of anions were calculated from those of the corresponding cation. RSD relative standard deviation

Table 2 Figures of merit of fluorescent methods for determination of Ag⁺

Materials used	Detection range(s), LOD(s)	Buffer/pH value	General advantages/disadvantages	Applicability to specific problems	Ref
silver(I)-specific DNA, Sybr green I	1–100 nM, 1 nM	MOPS buffer (100 mM, containing 500 mM NaNO ₃ , pH 6.90)	simple, cost-effective, label free, fast	detect Ag ⁺ in river water	[42]
GO, FAM labeled silver-specific DNA	0–200 nM, 5 nM	MOPS buffer (10 mM, containing NaNO ₃ , pH 7.0)	simple/ requires DNA labeling	detect Ag ⁺ in spiked sample and river water	[23]
nano-graphite, DNaseI, ROX-labeled C-rich ssDNA	0–800 nM, 0.3 nM	MOPS buffer (containing 100 mM NaNO ₃ , 2 mM Mg(NO ₃) ₂ , pH 7.0)	simple/ requires DNA labeling	detect Ag ⁺ in river water samples	[14]
silver (I) specific DNA, Thioflavine T	30–450 nM, ~16 nM	HEPES buffer (10 mM, pH 7.0)	simple, label free, fast	can also be used to detect amino acids such as Cys	[43]
CNPs, ROX dye-labeled ssDNA	0–400 nM, 500 pM	MOPS buffer (containing 50 mM NaNO ₃ , pH 7.0)	very low detection limit/requires DNA labeling	detect Ag ⁺ in lake water	[22]
quantum dots, C-rich ssDNA, Ru complex	0–16 μM, 100 nM	HEPES-NaOH buffer (10 mM, pH 7.4)	label free, simple, cost-effective	can in principle be used to detect other metal ions	[44]
Sybr green I, repeats of 20 C nucleotides	50–700 nM, 32 nM	MOPS buffer (20 mM, containing NaNO ₃ , pH 7.0)	simple, cost-effective, rapid (within 10 min)	sensing of spiked Ag ⁺ in drinking water, detect Ag nanoparticles	[45]
FAM labeled C-rich DNA	0.005–5 μM, 5 nM	MOPS buffer (containing 50 mM NaNO ₃ , pH 7.0)	simple, cost-effective, fast/requires DNA labeling, no linear correlation obtained	help to improve the direct Ag ⁺ detection in the environment	[46]
Sybr green I, Ag ⁺ -specific C-rich DNA	10–600 nM, 4.3 nM	MOPS buffer (20 mM, pH 7.2)	label free, cost-effective	determine Ag ⁺ in (spiked) water samples	[47]
nano-C60, FAM-labeled Ag ⁺ -specific DNA	0–300 nM, 1 nM	MOPS buffer (containing 50 mM NaNO ₃ , pH 7.0)	nano-C60 was firstly used as a sensing platform for fluorescent Ag ⁺ detection/requires DNA labeling	determine Ag ⁺ in spiked lake water sample	[48]
cationic perylene derivative, C-rich ssDNA	0–1000 nM, 5 nM	MOPS buffer (5 mM, containing 20 mM NaNO ₃ , pH 7.0)	label free, simple, fast, inexpensive, convenient	determine Ag ⁺ in spiked lake water sample	[49]
FAM-labeled C-rich ssDNA, label-free C-rich ssDNA	0–1 μM, 3.5 nM	HEPES buffer (10 mM, containing 200 mM NaNO ₃ , pH 7.4)	dual-output for Ag ⁺ and Cys detection, cost-effective, simple, fast/requires DNA labeling	determine Ag ⁺ in tap water and river water samples	[50]
SWCNT, FAM-labeled C-rich ssDNA	0–150 nM, 1 nM	HEPES buffer (10 mM HEPES, 200 mM NaNO ₃ , pH 7.4)	simple, effective, reusable/requires DNA labeling	can in principle be used to detect other metal ions	[51]
silver-specific DNA, AuNPs, Rhodamine B	2.73–1500 ppb, (25.31–13,905 nM) 2.73 ppb (25.31 nM)	MOPS buffer (10 mM, pH 7.0)	label free, relative wider analytical range	determine Ag ⁺ in spiked water samples, can in principle be used to detect other metal ions	this work

* FAM stands for carboxyfluorescein, C for cytosine, ssDNA for single-stranded DNA, GO for graphene oxide, CNPs for carbon nanoparticles, Cys for cysteine, AuNPs for gold nanoparticles, SWCNT for single-walled carbon nanotube. The Ru complex is Ru(bpy)₃dppz²⁺ (bpy=2,2'-bipyridine; dppz=dipyrido[3,2-a:2'-c]phenazine).

organic compounds cause no interference even at high concentration. As for Cl^- and HS^- , even the concomitant Cl^- achieves the high concentration of 50 ppm, Ag^+ could still be identified; In contrast, concomitant HS^- of 5 ppm can inhibit the response of the assay, but the inhibiting effect could be screening out by treated with nitric acid of appropriate concentration. More effective approach should be exploited to remove the HS^- of high concentration when employed this assay in real sample detection.

Detection of Ag^+ in water samples

The application of the present assay was evaluated for the determination of Ag^+ in several spiked water samples containing different concentrations of Ag^+ and some other metal cations and anions. The results are summarized in Table 1, which display that the mean recovery of samples was in the range of 99.9–102.7 % and the relative standard deviation (RSD) was between 3.49 and 5.21 %. The results reveal the potential application of this assay for Ag^+ detection in water samples.

Conclusions

In conclusion, a fluorescent assay for Ag^+ detection based on the aggregation of gold nanoparticles caused by silver-specific DNA and its effect on the fluorescence of Rhodamine B was established. The random coil cytosine-rich silver-specific DNA undergoes structural transformation upon capturing Ag^+ , mediating the dispersion/aggregation status of the gold nanoparticles, which at the same time affects the fluorescence intensity of Rhodamine B. As there was a positive correlation between the fluorescence intensity of the Rhodamine B and the involved amount of Ag^+ , an “off-on” type fluorescent method was thus developed. By monitoring the fluorescence intensity changes upon addition of Ag^+ , the Ag^+ could be selectively detected from 2.73 to 1500 ppb, with a detection limit of 2.73 ppb. Feasibility in determining spiked water samples was also demonstrated, suggesting this assay holds great practicality for Ag^+ detection in real matrices such as tablets, injections or drinking water. Compared with those existing fluorescent methods for Ag^+ determination, this assay possesses several superiorities such as requires no DNA labeling, relative wider analytical range, and can in principle be used to detect other metal ions by substituting the silver-specific DNA with other native or artificial bases that selectively bind to other metal ions (Table 2).

Acknowledgments This work was supported by the National High Technology Research and Development Program (“863” Program) of China (No. 2012AA101405), the Special Fund for Agro-scientific Research in the Public Interest of China (No. 201503149), the National Natural Science Foundation of China (Nos 31071860 and 20977062), the Municipal Natural Science Foundation of Shanghai, China

(13ZR1421700), and the Morningstar Fund of Shanghai Jiaotong University (No. 13X100010018).

References

- Li M, Gou H, Al Ogaidi I, Wu N (2013) Nanostructured sensors for detection of heavy metals: a review. *ACS Sustainable Chem Eng* 1(7):713–723
- Park J, Choi W, Jang K, Na S (2013) High-sensitivity detection of silver ions using oligonucleotide-immobilized oscillator. *Biosens Bioelectron* 41:471–476
- Liu B, Tan H, Chen Y (2013) Visual detection of silver (I) ions by a chromogenic reaction catalyzed by gold nanoparticles. *Microchim Acta* 180(5–6):331–339
- Zhang JF, Zhou Y, Yoon J, Kim JS (2011) Recent progress in fluorescent and colorimetric chemosensors for detection of precious metal ions (silver, gold and platinum ions). *Chem Soc Rev* 40(7):3416–3429
- Hidalgo E, Dominguez C (1998) Study of cytotoxicity mechanisms of silver nitrate in human dermal fibroblasts. *Toxicol Lett* 98(3):169–179
- Kumar M, Kumar R, Bhalla V (2010) Optical chemosensor for Ag^+ , Fe^{3+} , and cysteine: information processing at molecular level. *Org Lett* 13(3):366–369
- Ratte HT (1999) Bioaccumulation and toxicity of silver compounds: a review. *Environ Toxicol Chem* 18(1):89–108
- Pu Q, Sun Q (1998) Application of 2-mercaptobenzothiazole-modified silica gel to on-line preconcentration and separation of silver for its atomic absorption spectrometric determination. *Analyst* 123(2):239–243
- Manzoori JL, Abdolmohammad-Zadeh H, Amjadi M (2007) Ultra-trace determination of silver in water samples by electrothermal atomic absorption spectrometry after preconcentration with a ligand-less cloud point extraction methodology. *J Hazard Mater* 144(1–2):458–463
- Wang T, Jia X, Wu J (2003) Direct determination of metals in organics by inductively coupled plasma atomic emission spectrometry in aqueous matrices. *J Pharm Biomed* 33(4):639–646
- Mitrano DM, Barber A, Bednar A, Westerhoff P, Higgins CP, Ranville JF (2012) Silver nanoparticle characterization using single particle ICP-MS (SP-ICP-MS) and asymmetrical flow field flow fractionation ICP-MS (AF4-ICP-MS). *J Anal At Spectrom* 27(7):1131–1142
- Mohadesi A, Taher MA (2007) Stripping voltammetric determination of silver(I) at carbon paste electrode modified with 3-amino-2-mercapto quinazolin-4(3H)-one. *Talanta* 71(2):615–619
- Ceresa A, Radu A, Peper S, Bakker E, Pretsch E (2002) Rational design of potentiometric trace level ion sensors. A Ag^+ -selective electrode with a 100 ppt detection limit. *Anal Chem* 74(16):4027–4036
- Wei Y, Li B, Wang X, Duan Y (2014) Magnified fluorescence detection of silver(I) ion in aqueous solutions by using nano-graphite-DNA hybrid and DNase I. *Biosens Bioelectron* 58:276–281
- Zhou P, Wu YG, Zhan SS, Xu LR, Shi WW, Xi T, Zhan XJ (2011) A simple and label-free sensor for mercury(II) detection in aqueous solution by malachite green based on a resonance scattering spectral assay. *Chem Commun* 47(21):6027–6029
- Zhan S, Wu Y, Luo Y, Liu L, He L, Xing H, Zhou P (2014) Label-free fluorescent sensor for lead ion detection based on lead(II)-stabilized G-quadruplex formation. *Anal Biochem* 462:19–25
- Wu Y, Zhan S, Wang L, Zhou P (2014) Selection of a DNA aptamer for cadmium detection based on cationic polymer mediated aggregation of gold nanoparticles. *Analyst* 139(6):1550–1561

18. Liu J, Cao Z, Lu Y (2009) Functional nucleic acid sensors. *Chem Rev* 109(5):1948–1998
19. Zhan SS, Wu YG, He L, Wang FZ, Zhan XJ, Zhou P, Qiu SY (2012) A silver-specific DNA-based bio-assay for Ag(I) detection via the aggregation of unmodified gold nanoparticles in aqueous solution coupled with resonance Rayleigh scattering. *Anal Methods-Uk* 4(12):3997–4002
20. Ono A, Cao S, Togashi H, Tashiro M, Fujimoto T, Machinami T, Oda S, Miyake Y, Okamoto I, Tanaka Y (2008) Specific interactions between silver(I) ions and cytosine-cytosine pairs in DNA duplexes. *Chem Commun* 39:4825–4827
21. Li C, Yang Y, Zhang B, Chen G, Wang Z, Li G (2014) Conjugation of graphene oxide with DNA-modified gold nanoparticles to develop a novel colorimetric sensing platform. *Part Part Syst Charact* 31(2): 201–208
22. Li H, Zhai J, Sun X (2011) Sensitive and selective detection of silver (I) ion in aqueous solution using carbon nanoparticles as a cheap, effective fluorescent sensing platform. *Langmuir* 27(8):4305–4308
23. Wen Y, Xing F, He S, Song S, Wang L, Long Y, Li D, Fan C (2010) A graphene-based fluorescent nanoprobe for silver (I) ions detection by using graphene oxide and a silver-specific oligonucleotide. *Chem Commun* 46(15):2596–2598
24. Xie WY, Huang WT, Li NB, Luo HQ (2012) Design of a dual-output fluorescent DNA logic gate and detection of silver ions and cysteine based on graphene oxide. *Chem Commun* 48(1):82–84
25. Zhang Z, Yan J (2014) A signal-on electrochemical biosensor for sensitive detection of silver ion based on alkanethiol-carbon nanotube-oligonucleotide modified electrodes. *Sens Actuators B Chem* 202:1058–1064
26. Nolan EM, Lippard SJ (2008) Tools and tactics for the optical detection of mercuric ion. *Chem Rev* 108(9):3443–3480
27. Zhou Y, Xu Z, Yoon J (2011) Fluorescent and colorimetric chemosensors for detection of nucleotides, FAD and NADH: highlighted research during 2004–2010. *Chem Soc Rev* 40(5): 2222–2235
28. Azam A, Chawla H, Pandey S (2010) A novel dansyl-appended glycoluril-based fluorescence sensor for silver ions. *Tetrahedron Lett* 51(36):4710–4711
29. Huang S, He S, Lu Y, Wei F, Zeng X, Zhao L (2011) Highly sensitive and selective fluorescent chemosensor for Ag⁺ based on a coumarin-Se2N chelating conjugate. *Chem Commun* 47(8):2408–2410
30. Xu L, Xu Y, Zhu W, Yang C, Han L, Qian X (2012) A highly selective and sensitive fluorescence “turn-on” probe for Ag⁺ in aqueous solution and live cells. *Dalton T* 41(24):7212–7217
31. Zhan S, Yu M, Lv J, Wang L, Zhou P (2014) Colorimetric detection of trace arsenic(III) in aqueous solution using arsenic aptamer and gold nanoparticles. *Aust J Chem* 67(5):813–818
32. Zhang XB, Kong RM, Lu Y (2011) Metal ion sensors based on DNazymes and related DNA molecules. *Annu Rev Anal Chem (Palo Alto, Calif)* 4(1):105–128
33. Zhang H, Wang L, Jiang W (2011) Label free DNA detection based on gold nanoparticles quenching fluorescence of Rhodamine B. *Talanta* 85(1):725–729
34. Li HB, Chen F, Xu XR (2000) Fluorimetric determination of methylmercury as an ion-association complex with rhodamine B in the presence of iodide. *Fresenius J Anal Chem* 367(5):499–501
35. Huang CC, Chang HT (2006) Selective gold-nanoparticle-based “turn-on” fluorescent sensors for detection of mercury(II) in aqueous solution. *Anal Chem* 78(24):8332–8338
36. Shang L, Jin L, Dong S (2009) Sensitive turn-on fluorescent detection of cyanide based on the dissolution of fluorophore functionalized gold nanoparticles. *Chem Commun* 45(21):3077–3079
37. Pylaev T, Volkova E, Kochubey V, Bogatyrev V, Khlebtsov N (2013) DNA detection assay based on fluorescence quenching of rhodamine B by gold nanoparticles: the optical mechanisms. *J Quant Spectrosc Radiat Transf* 131:34–42
38. Berezin MY, Achilefu S (2010) Fluorescence lifetime measurements and biological imaging. *Chem Rev* 110(5):2641–2684
39. Zhan S, Wu Y, Liu L, Xing H, He L, Zhan X, Luo Y, Zhou P (2013) A simple fluorescent assay for lead (II) detection based on lead (II)-stabilized G-quadruplex formation. *RSC Adv* 3(38):16962–16966
40. Wang FZ, Wu YG, Zhan SS, He L, Zhi WT, Zhou XX, Zhou P (2013) A simple and sensitive colorimetric detection of silver ions based on cationic polymer-directed AuNPs aggregation. *Aust J Chem* 66(1):113–118
41. Lin CY, Yu CJ, Lin YH, Tseng WL (2010) Colorimetric sensing of silver(I) and mercury(II) ions based on an assembly of tween 20-stabilized gold nanoparticles. *Anal Chem* 82(16):6830–6837
42. Yang Q, Li F, Huang Y, Xu H, Tang L, Wang L, Fan C (2013) Highly sensitive and selective detection of silver (I) in aqueous solution with silver (I)-specific DNA and Sybr green I. *Analyst* 138(7):2057–2060
43. Wang Y, Geng F, Xu H, Qu P, Zhou X, Xu M (2012) A label-free oligonucleotide based thioflavin-T fluorescent switch for Ag⁺ detection with low background emission. *J Fluoresc* 22(3):925–929
44. Sun W, Yao J, Yao T, Shi S (2013) Label-free fluorescent DNA sensor for the detection of silver ions based on molecular light switch Ru complex and unmodified quantum dots. *Analyst* 138(2):421–424
45. Lin YH, Tseng WL (2009) Highly sensitive and selective detection of silver ions and silver nanoparticles in aqueous solution using an oligonucleotide-based fluorogenic probe. *Chem Commun* 45(43): 6619–6621
46. Wang L, Tian J, Li H, Zhang Y, Sun X (2011) A novel single-labeled fluorescent oligonucleotide probe for silver (I) ion detection based on the inherent quenching ability of deoxyguanosines. *Analyst* 136(5): 891–893
47. Pu W, Zhao H, Huang C, Wu L, Xua D (2012) Fluorescent detection of silver (I) and cysteine using SYBR Green I and a silver (I)-specific oligonucleotide. *Microchim Acta* 177(1–2):137–144
48. Li H, Zhai J, Sun X (2011) Highly sensitive and selective detection of silver (I) ion using nano-C60 as an effective fluorescent sensing platform. *Analyst* 136(10):2040–2043
49. Yang Y, Li W, Qi H, Zhang Q, Chen J, Wang Y, Wang B, Wang S, Yu C (2012) Detection of silver(I) ions based on the controlled self-assembly of a perylene fluorescence probe. *Anal Biochem* 430(1): 48–52
50. Xie WY, Huang WT, Li NB, Luo HQ (2011) Silver(I) ions and cysteine detection based on photoinduced electron transfer mediated by cytosine-Ag⁺-cytosine base pairs. *Analyst* 136(20):4130–4133
51. Zhao C, Qu K, Song Y, Xu C, Ren J, Qu X (2010) A reusable DNA single-walled carbon-nanotube-based fluorescent sensor for highly sensitive and selective detection of Ag⁺ and cysteine in aqueous solutions. *Chem Eur J* 16(27):8147–8154